Electron-impact excitation of krypton

G. D. Meneses
Instituto de Fisica "Gleb Wataghin," Universidade Estadual de Campinas, 13100 Campinas, São Paulo, Brazil

F. J. da Paixão*
Joint Institute for Laboratory Astrophysics, University of Colorado and National Bureau of Standards, Boulder, Colorado 80309

N. T. Padial
Institute for Modern Optics, Department of Physics and Astronomy, University of New Mexico, Albuquerque, New Mexico 87131
(Received 12 November 1984; revised manuscript received 15 April 1985)

First-order many-body theory has been used to calculate the differential, integrated, and momentum-transfer cross sections for the electron-impact excitation of the $5s'[\frac{1}{2}]_1^0(^1P_1)$, $5s[\frac{3}{2}]_1^0(^3P_1)$, $5s'[\frac{1}{2}]_0^0(^3P_0)$, and $5s[\frac{3}{2}]_2^0(^3P_2)$ states of krypton for the incident energies of 20, 30, 50, 60, and 100 eV. Electron-photon coincidence parameters for the optically allowed states have been obtained. The results are compared to available experimental results.

I. INTRODUCTION

The study of electron-impact excitation of rare-gas atoms dates from the second decade of this century. Due to their chemical inactivity, the rare gases could easily be handled and were preferred by the experimentalists. Among those early experiments, we find the first observation of the integrated cross section (ICS) of Kr by Ramsauer[1] and by Ramsauer and Kollath.[2] Later, Lewis *et al.*[3] measured the differential cross section (DCS) but were unable to resolve the fine structure of the $4p \rightarrow 5s$ transition. Delage and Carrete[4] observed the fine structure of the state although they could not normalize their results. Only recently have absolute DCS's (Ref. 5) been obtained for several states of Kr. Much less attention has been given to the theoretical aspects of the problem. The calculations of Ganas and Green[6] of the ICS for the $4p \rightarrow 5s$ optically allowed transition are the only work reported in the literature. They used a Born-type approximation with semiempirical angular distortion.

The electron-photon coincidence experiments[7] (EPCE) have greatly aided the understanding of the excitation process in atoms. The theoretical analysis shows that direct information about the scattering amplitudes can be obtained from these measurements. A large amount of experimental and theoretical work[7] has been dedicated to the subject. In the case of *LS*-coupled systems (e.g., helium) two parameters, usually λ and χ,[8] can be extracted from the experiments. The λ and χ parameters give the ratio of the differential cross sections and the relative phase of the scattering amplitude for the magnetic sublevels, respectively. When the spin-orbit interaction is considered for the atomic excited states, the experiments allow the determination of four parameters, e.g., λ, $\bar{\chi}$, ϵ, and Δ.[9]

Recently, McGregor *et al.*,[10] Nishimura *et al.*,[11] and Crowe *et al.*[12] reported electron-photon coincidence parameters (EPCP) for Kr which should provide an ideal test for different theoretical treatments. Nevertheless, since these experiments disagree with each other, a greater burden is placed on the theoretical findings. Both the DCS and EPCP for Kr were measured in the intermediate-energy region which extends from a few electron volts above the ionization threshold to the point at which the first Born approximation (FBA) is valid. In this energy range such simple models as the distorted-wave approximation (DWA) and the first-order many-body theory[13] (FOMBT) give good results for the DCS of the optically allowed transitions. More rigorous approaches such as the close-coupling[14] (CC) method are very accurate in the threshold energy region; however, such treatments become extremely complicated and expensive to apply at higher energies, especially for heavy atoms. Krypton with 36 electrons would pose serious complications for a CC treatment, thus necessitating a more approximate approach.[15] Previous applications of the FOMBT to the calculation of the DCS of He,[16–19] Ne,[20,21] and Ar (Refs. 22 and 23) provided results in good agreement with the experiment for the optically allowed transition and of the correct order of magnitude for cases described only by exchange processes.

We used the FOMBT, modified to include spin-orbit effects in the target,[22] to calculate the DCS and EPCP of Kr. We were motivated to make the present study by the lack of other theoretical results. In addition, krypton is the first of the noble gases with *d* electrons, which are responsible for magnetic properties in transition metals, to be studied with the FOMBT. Finally, since the spin-orbit interaction is more important for larger atoms, the krypton system provides a more stringent test of the way we incorporated these effects into the theory.

The plan of this paper is the following. In Sec. II, we present a summary of the FOMBT in the calculation of the DCS and the EPCP for atoms with spin-orbit coupling; in Sec. III we discuss details of the calculations and comment about the computer codes used. The results are presented in Sec. IV.

II. THEORY

A. The FOMBT

The FOMBT and its extension to include spin-orbit effects in the target have been discussed in detail in Ref. 22. In this subsection we present only a summary of the theory.

The FOMBT in its original form is a nonrelativistic theory, appropriate for the study of systems for which the total angular momentum L and the total spin S are good quantum numbers. The T matrix describing the excitation process has two parts, the direct T^D_{LMS} and the exchange T^E_{LMS} terms, given by

$$T^D_{LMS}=\int d\mathbf{r}_1\, d\mathbf{r}_2 f_{\mathbf{q}}^{(-)*}(\mathbf{r}_1) f_{\mathbf{p}}^{(+)}(\mathbf{r}_1) \times V(\mathbf{r}_1-\mathbf{r}_2)\tilde{X}_n(\mathbf{r}_2,\mathbf{r}_2)\ , \tag{1}$$

$$T^E_{LMS}=\int d\mathbf{r}_1\, d\mathbf{r}_2 (f_{\mathbf{q}}^{(-)})^*(\mathbf{r}_1) f_{\mathbf{p}}^{(+)}(\mathbf{r}_2) \times V(\mathbf{r}_1-\mathbf{r}_2)\tilde{X}_n(\mathbf{r}_2,\mathbf{r}_1)\ , \tag{2}$$

where $f_{\mathbf{p}}^{(+)}$ and $f_{\mathbf{q}}^{(-)}$ represent the incoming and outgoing electron orbitals, calculated in the field of the ground state, with momenta $\mathbf{p}$ and $\mathbf{q}$, respectively. The Coulomb potential is given by $V(\mathbf{r}_1-\mathbf{r}_2)$ and the transition density matrix, which in the Hartree-Fock approximation is simply a product of two orbitals, by $\tilde{X}_n(\mathbf{r}_1,\mathbf{r}_2)$.

The introduction of the spin-orbit interaction has two major effects. The first occurs in the target, where states with the same value of J, formed by the coupling of L and S, are mixed, dramatically affecting some of the properties associated with the state. For example, a ^3P state with a dipole-forbidden transition to the ground state is transformed to an optically allowed state due to the mixing of the ^1P component. The second effect occurs in the description of the continuum electron. The spin-orbit interaction between the continuum electron and the atom can polarize an initially unpolarized electron beam; however, we expect from spin-polarization measurements that this effect will not be very large for e-Kr scattering.[24]

In our calculations we consider the spin-orbit potential only in the target. Through a recoupling of the angular momenta, we can transform the transition density matrix from the L,S to the L,S,J description:

$$\tilde{X}_{n,L,S,J}(\mathbf{r}_1,\mathbf{r}_2)=\sum_{M_S,M_L} C^{SLJ}_{M_S M_L M_J}\tilde{X}^{L,S}_{n,M_L,M_S}(\mathbf{r}_1,\mathbf{r}_2)\ , \tag{3}$$

where $C^{SLJ}_{M_S M_L M_J}$ is a Clebsch-Gordan coefficient. In this case we have the transformations $^1P\rightarrow{}^1P_1$ and $^3P\rightarrow{}^3P_{2,1,0}$.

The states with $J=1$ are mixed, and the coefficients are determined in the scheme suggested by Cowan and Andrew:[25]

$$|\,5s'[\tfrac{1}{2}]^0_1(^1P_1)\rangle=-a\,|\,5\,^1P\rangle+b\,|\,5\,^3P\rangle\ , \tag{4a}$$

$$|\,5s[\tfrac{3}{2}]^0_1(^3P_1)\rangle=b\,|\,5\,^1P\rangle+a\,|\,5\,^3P\rangle\ , \tag{4b}$$

where $a=0.683$ and $b=0.730$. McConnell and Moiseiwitsch[26] used a similar approach in the study of the excitation of Hg, in which they reduced an N electron to a two-electron problem by incorporating the spin-orbit effects only in the $6p$ state. For the noble gas, the transition density matrix approach transforms the N electrons to a particle and a hole problem.

B. The cross sections

Using the transition density matrices in the L,S,J description, we obtain the T matrices as functions of $T^D_{L,M,S}$ and $T^E_{L,M,S}$ for the excitation of each $5s[j]^0_J$ state, where $j=\frac{1}{2}$ and $\frac{3}{2}$ and $J=0$, 1, and 2. We simplify our notation as follows:

$$T^D_{L=1,M_L,S=0}\rightarrow T^{SD}_{M_L}\ ,$$

$$T^E_{L=1,M_L,S=0}\rightarrow T^{SE}_{M_L}\ ,$$

$$T^E_{L=1,M_L,S=1}\rightarrow T^{TE}_{M_L}\ .$$

Using this notation, we can write the differential cross sections for each level[22] as

$$\left(\frac{d\sigma}{d\Omega}\right)_{5s'[\frac{1}{2}]^0_1}=\sigma_0(5s'[\tfrac{1}{2}]^0_1)+2\sigma_1(5s'[\tfrac{1}{2}]^0_1\ , \tag{5a}$$

$$\left(\frac{d\sigma}{d\Omega}\right)_{5s[\frac{3}{2}]^0_1}=\sigma_0(5s[\tfrac{3}{2}]^0_1)+2\sigma_1(5s[\tfrac{3}{2}]^0_1)\ , \tag{5b}$$

$$\left(\frac{d\sigma}{d\Omega}\right)_{5s'[\frac{1}{2}]^0_0}=\frac{1}{4\pi^2}\frac{q}{p}\frac{1}{6}(2\,|\,T^{TE}_1\,|^2+|\,T^{TE}_0\,|^2)\ , \tag{5c}$$

$$\left(\frac{d\sigma}{d\Omega}\right)_{5s[\frac{3}{2}]^0_2}=\frac{1}{4\pi^2}\frac{q}{p}\frac{5}{6}(2\,|\,T^{TE}_1\,|^2+|\,T^{TE}_0\,|^2)\ , \tag{5d}$$

where $\sigma_0(5s[j]^0_J)$ and $\sigma_1(5s[j]^0_J)$ are the differential cross sections for the excitation of the magnetic sublevels 0 and 1, respectively. For the state $5s'[\frac{1}{2}]^0_1$, σ_0 and σ_1 are

$$\sigma_0=\frac{1}{4\pi^2}\frac{q}{p}\left[\frac{b^2}{2}\,|\,2T^{SD}_0-T^{SE}_0\,|^2+\frac{a^2}{2}\,|\,T^{TE}_1\,|^2\right] \tag{6a}$$

and

$$\sigma_1=\frac{1}{4\pi^2}\frac{q}{p}\left[\frac{b^2}{2}\,|\,2T^{SD}_1-T^{SE}_1\,|^2+\frac{a^2}{4}\,|\,T^{TE}_0\,|^2+\frac{a^2}{4}\,|\,T^{TE}_1\,|^2\right]. \tag{6b}$$

For the state $5s[\frac{3}{2}]^0_1$, the formulas are analogous, with a and b interchanged.

C. The electron-photon coincidence parameters

The electron-photon coincidence parameters, λ, $\overline{\chi}$, ϵ, and Δ, defined by da Paixão *et al.*[9] have been discussed in detail in Ref. 23. We can write the expressions for these parameters as functions of σ_0, σ_1 and the T matrices for the state $5s'[\frac{1}{2}]^0_1$ as follows:

$$\lambda=\frac{\sigma_0}{\sigma_0+2\sigma_1}\ , \tag{7a}$$

$$\cos\Delta=\frac{\frac{1}{4\pi^2}\frac{q}{p}\left|\left[\frac{b^2}{2}(2T_0^{SD}-T_0^{SE})^*(2T_1^{SD}-T_1^{SE})-\frac{a^2}{4}T_0^{TE*}T_1^{TE}\right]\right|}{(\sigma_0\sigma_1)^{1/2}}\ , \tag{7b}$$

$$\cos\bar{\chi}=\frac{\mathrm{Re}\left[\frac{b^2}{2}(2T_0^{SD}-T_0^{SE})^*(2T_1^{SD}-T_1^{SE})-\frac{a^2}{4}T_0^{TE*}T_1^{TE}\right]}{\left|\left[\frac{b^2}{2}(2T_0^{SD}-T_0^{TE})^*(2T_1^{SD}-T_1^{SE})-\frac{a^2}{4}T_0^{TE*}T_1^{TE}\right]\right|}\ , \tag{7c}$$

$$\cos\chi=\cos\Delta\cos\bar{\chi}\ , \tag{7d}$$

$$\cos\epsilon=\frac{\frac{1}{4\pi^2}\frac{q}{p}\left[\frac{b^2}{2}|2T_1^{SD}-T_1^{SE}|^2-\frac{a^2}{4}|T_1^{TE}|^2\right]}{\sigma_1}\ . \tag{7e}$$

For the state $5s[\frac{3}{2}]_1^0$, the formulas are analogous, with a and b interchanged.

III. DETAILS OF THE CALCULATIONS

A. The angular momentum analysis

The T matrices from Eqs. (1) and (2) can be written[22] as partial wave expansions:

$$T^D_{LM_LS}=\frac{4\pi}{pq}\sum_{l''\geq|M_L|}\sum_{l'=l''-1}^{l''+1}\frac{(-1)^{(l'-l''+1)/2}}{\sqrt{3}}(-i)\exp\{i[\sigma_{l'}(p)+\sigma_{l''}(q)]\}$$
$$\times(2l'+1)(2l''+1)\left[\frac{(l''-M_L)!}{(l''+M_L)!}\right]\begin{bmatrix}l' & l'' & 1\\ 0 & 0 & 0\end{bmatrix}\begin{bmatrix}l' & l'' & 1\\ 0 & -M_L & M_L\end{bmatrix}$$
$$\times\cos\delta_{l'}(p)\cos\delta_{l''}(q)I^{p,q}_{l'l''S}P_{l''}^{M_L}(\cos\theta_q)\equiv\sum_{l''}T^D_{l''}P_{l''}^{M_L}(\cos\theta_q)\ , \tag{8a}$$

where

$$I^{pq}_{l'l''S}\equiv\int_0^\infty dr_1\int_0^\infty dr_2\mu_{l''}(q,r_1)\mu_{l'}(p,r_1)\frac{r_<}{r_>^2}R_{4p}(r_2)R_{5s}(r_2) \tag{8b}$$

and

$$T^E_{LM_LS}=\frac{4\pi}{pq}\sum_{l''\geq|M_L|}\sum_{l'=l''-1}^{l''+1}(-1)^{(l'+l''+1)/2}(-i)\sqrt{3}(2l''+1)\exp\{i[\delta_{l'}(p)+\delta_{l''}(q)]\}$$
$$\times\left[\frac{(l''-M_L)!}{(l''+M_L)!}\right]\begin{bmatrix}l' & l'' & 1\\ 0 & 0 & 0\end{bmatrix}\begin{bmatrix}l'' & l' & 1\\ M_L & 0 & -M_L\end{bmatrix}$$
$$\times\cos\delta_{l'}(p)\cos\delta_{l''}(q)J^{pq}_{l'l''S}P_{l''}^{M_L}(\cos\theta_q)\equiv\sum_{l''}T^E_{l''}P_{l''}^{M_L}(\cos\theta_q)\ , \tag{9a}$$

where

$$J^{pq}_{l'l''S}\equiv\int_0^\infty dr_1\int_0^\infty dr_2\mu_{l''}(q,r_2)\mu_{l'}(p,r_1)\frac{r_<^{l'}}{r_>^{l'+1}}R_{4P}(r_2)R_{5s}(r_1)\ . \tag{9b}$$

In the expressions (8a), (8b) and (9a), (9b), δ_l is the lth partial-wave phase shift, θ_q is the scattering angle, and $\mu_l(p,r)$ is the continuum radial function. R_{4p} and R_{5s} are the radial parts of the $4p$ and $5s$ orbitals of the atom, respectively.

In the numerical calculation of these expressions we must truncate the sums at a finite value l_D. The expansion of T^E requires only a small number of partial waves to converge. In this case the appropriate value of l_D, which depends on the incident electron energy E_i, changes

from $l_D=6$ at $E_i=15$ eV to $l_D=12$ at $E_i=100$ eV. The sum over l'' in the expansion of T^D is much more slowly convergent, and the required value of l_D would be quite large ($l_D>100$). However, for $l'>l_D$, the FBA becomes valid, allowing us to complete the sum for $l_D<l''<\infty$. This can be easily done if we write $T^D_{LM_LS}$ in the rearranged form

$$T^D_{LM_LS}=\sum_{l''\geq|M_L|}^{l_D} T^D_{l''}P^{M_L}_{l''}(\cos\theta_q)+T^{\mathrm{FBA}}_{LM_LS} - \sum_{l''\geq|M_L|}^{l_D} T^{\mathrm{FBA}}_{l''}P^{M_L}_{l''}(\cos\theta_q)\,,$$

where $T^{\mathrm{FBA}}_{LM_LS}$ is the closed-form expression for $T^D_{LM_LS}$ in the FBA. The second sum in Eq. (10) is the partial-wave expansion of $T^D_{LM_LS}$ in the FBA.

Accurate numerical techniques were used to calculate the radial integrals $I^{pq}_{l'l''S}$ and $J^{pq}_{l'l''S}$. To converge $J^{pq}_{l'l''S}$, we carried out the integration until $R_0=70$ a.u. The long-range nature of $I^{pq}_{l'l''S}$ required the integration to be made until $R_1=270$ a.u. In this case, in the interval $R_0<r\leq R_1$ the continuum orbitals were replaced by the exact asymptotic functions.

B. The computer codes

We calculated the bound-state orbital using the code of Froese-Fischer[27] (MCHF77). We obtained the ground state in a single-configuration calculation and the excited bound state in the "frozen core" approximation. The accuracy of the bound-state wave functions were checked against the oscillator strength to the $^1P_1\rightarrow{}^1S_0$ transition measured by de Jongh and van Eck.[28] Our result is 0.144, compared with 0.14 ± 0.015 given by the experiments. The continuum Hartree-Fock orbitals were obtained using a modified version of a computer code by Bates.[29] One of the modifications made to this code allows us to consider exchange for only some partial waves. Also, we can now fit the continuum orbital to the exact asymptotic wave function, therefore reducing the integration to just beyond the extent of the exchange contribution. To avoid overflows, some minor modifications were necessary, including a different initial estimate for the solution of our equations. We programmed simple procedures for the calculation of the T matrices, the cross sections, and the EPCP.

IV. RESULTS AND DISCUSSIONS

We present in Fig. 1 the static-exchange phase shifts for the s, p, d, and f partial waves. To test our modifications of the Bates program, we have also calculated the phase shifts using the linear algebraic code of Collins and Schneider.[30] In this case we used the ground-state wave function by Clementi and Roetti.[31] Both sets of results agree to better than 0.1% for low partial waves ($l=0$, 1, and 2). Although the difference increases for higher partial waves for which the phase shifts are small, the cross section is insensitive to these components.

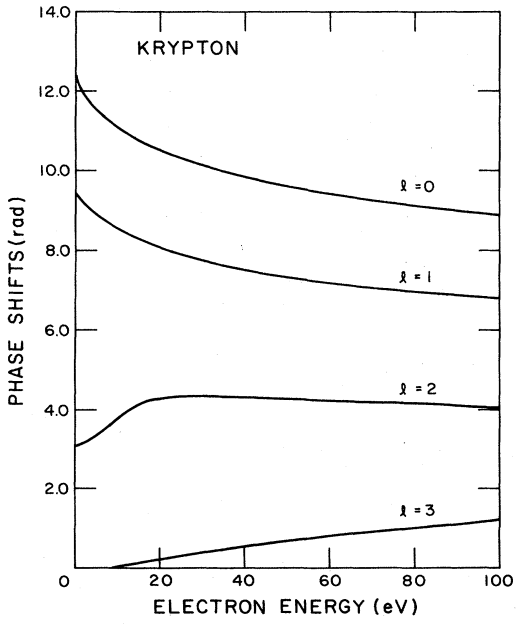

FIG. 1. Phase shifts for s, p, d, and f partial waves.

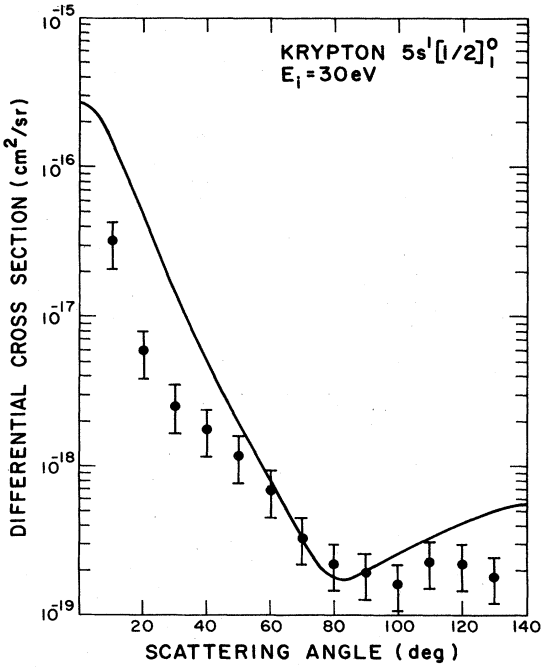

FIG. 2. DCS for the excitation of the $5s'[\frac{1}{2}]^0_1$ state of krypton at 30 eV. The measured data are from Trajmar *et al.* (Ref. 5).

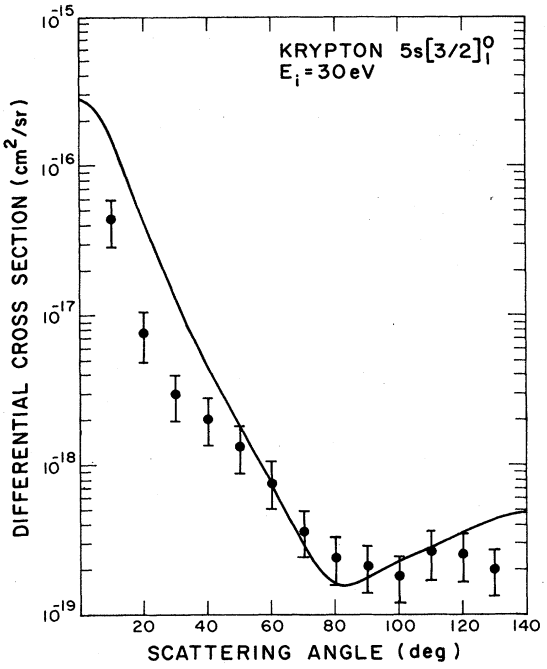

FIG. 3. DCS for the excitation of the $5s[\frac{3}{2}]^0_1$ state of krypton at 30 eV. The measured data are from Trajmar *et al.* (Ref. 5).

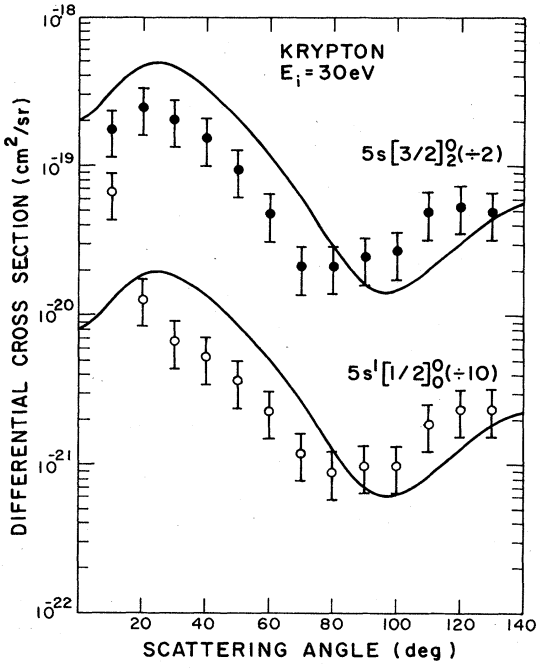

FIG. 4. DCS for the excitation of the $5s[\frac{3}{2}]^0_2$ and $5s'[\frac{1}{2}]^0_0$ states of krypton at 30 eV. The measured data are from Trajmar *et al.* (Ref. 5).

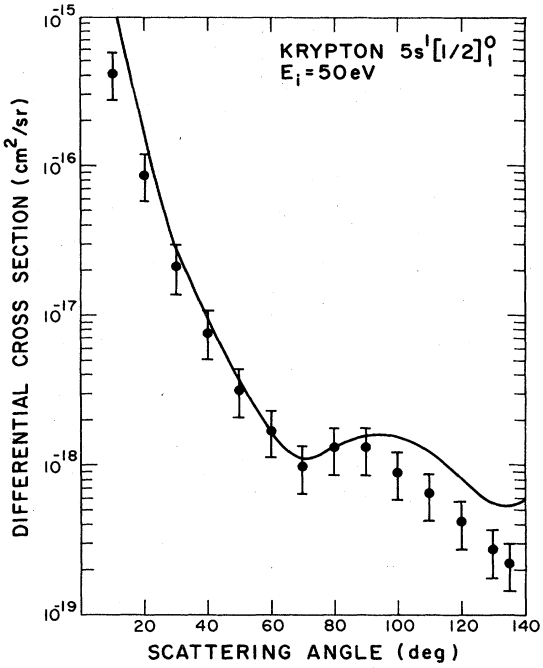

FIG. 5. As Fig. 2, for 50-eV incident electron energy.

A. The cross section

We calculated the FOMBT DCS for the excitation of the $5s'[\frac{1}{2}]^0_1$, $5d[\frac{3}{2}]^0_1$, $5s'[\frac{1}{2}]^0_0$, and $5s[\frac{3}{2}]^0_2$ states of Kr at the incident electron energies of 20, 30, 50, 60, and 100

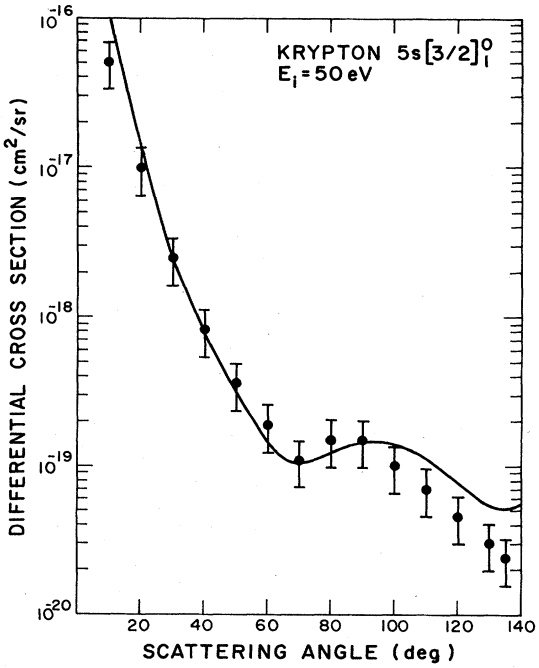

FIG. 6. As Fig. 3, for 50-eV incident electron energy.

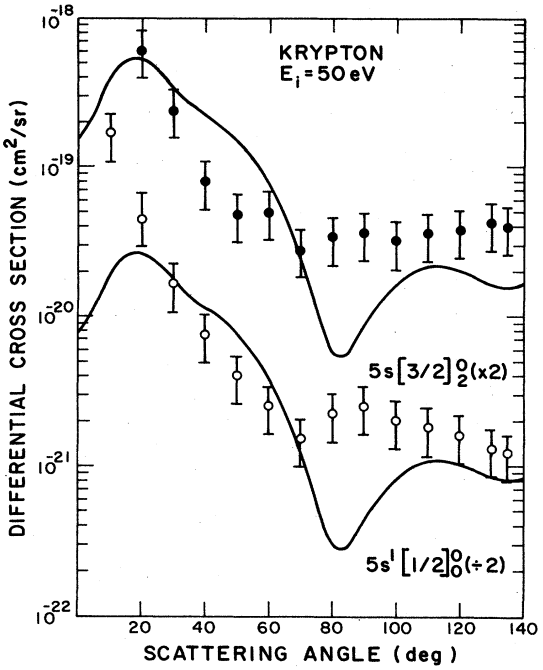

FIG. 7. As Fig. 4, for 50-eV incident electron energy.

eV. In Figs. 2–7 we compare our theoretical results at $E_i = 30$ and 50 eV with the experimental data of Trajmar *et al.*[5] (Tabled results can be obtained from the authors.)

For the optically allowed transitions ($\Delta J = 1$), the agreement of our present results with the experiment is comparable to that obtained for Ar (Ref. 22) although worse than for Ne.[20] In general, the FOMBT describes well these transitions, except at 20 eV where the theoretical results are too low by a factor that varies from 7 at 10° to 1.5 at 70°. The agreement with the experiment improves at 30 eV, with the results reasonably accurate in the angular range $50° \leq \theta \leq 120°$ and in better accord at smaller an-

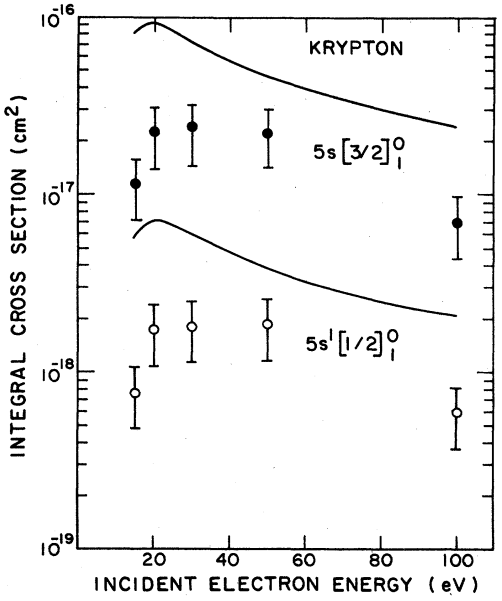

FIG. 8. ICS for the excitation of the $5s[\frac{3}{2}]^0_1$ and $5s'[\frac{1}{2}]^0_1$ states of krypton. The data points are from Ref. 5.

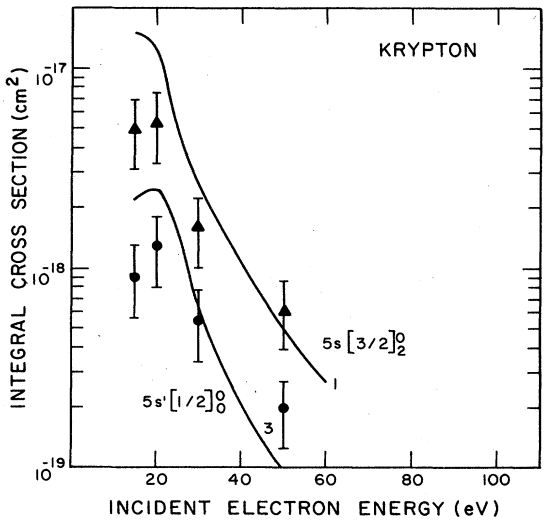

FIG. 9. As Fig. 8, for the $5s[\frac{3}{2}]^0_2$ and $5s'[\frac{1}{2}]^0_0$ states.

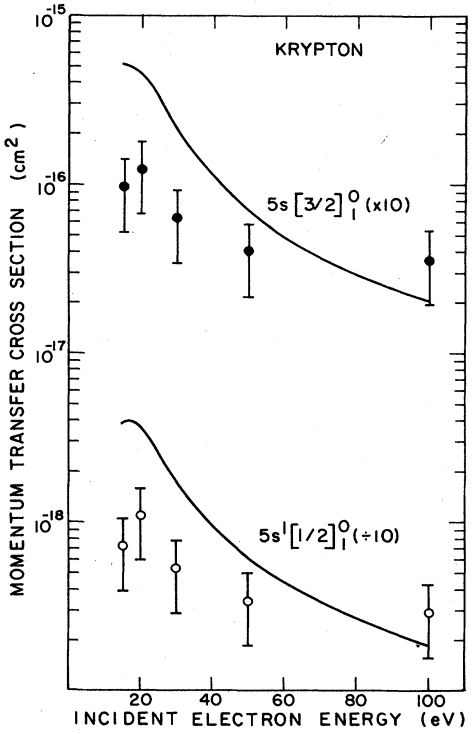

FIG. 10. Momentum-transfer cross section for the excitation of the $5s[\frac{3}{2}]^0_1$ and $5s'[\frac{1}{2}]^0_1$ states of krypton. The data points are from Ref. 5.

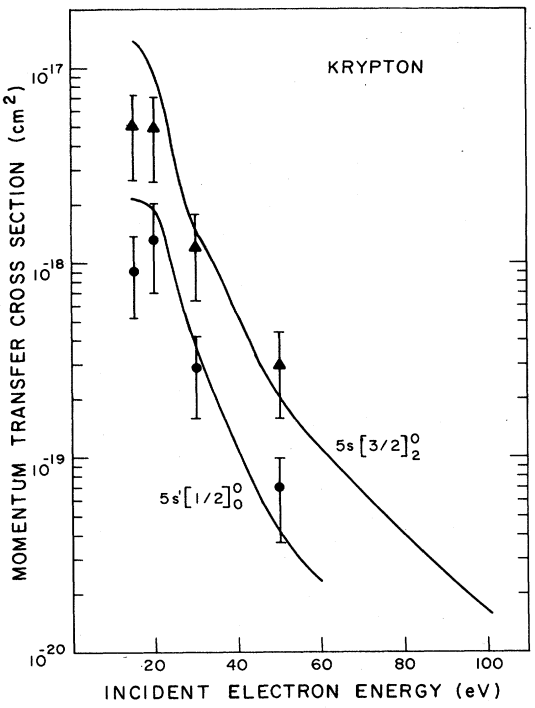

FIG. 11. As Fig. 10, for the $5s[\frac{3}{2}]_2^0$ and $5s'[\frac{1}{2}]_0^0$ states.

TABLE I. Parameter λ for excitation of $5s'[\frac{1}{2}]_1^0$ of krypton.

Angle (deg)	Incident energy 20 eV	30 eV	50 eV	60 eV	100 eV
0	0.997	0.999	1.000	1.000	1.000
10	0.935	0.795	0.517	0.423	0.239
20	0.865	0.713	0.564	0.543	0.700
30	0.870	0.824	0.914	0.968	0.568
40	0.903	0.938	0.884	0.735	0.111
50	0.884	0.894	0.494	0.260	0.103
60	0.800	0.690	0.111	0.042	0.269
70	0.719	0.390	0.134	0.246	0.245
80	0.713	0.276	0.416	0.422	0.272
90	0.736	0.502	0.561	0.588	0.449
100	0.463	0.592	0.643	0.767	0.339
110	0.263	0.530	0.741	0.898	0.145
120	0.215	0.401	0.890	0.945	0.194
130	0.219	0.291	0.927	0.717	0.364
140	0.252	0.238	0.588	0.373	0.616
150	0.320	0.248	0.318	0.285	0.538
160	0.451	0.339	0.263	0.375	0.467
170	0.671	0.592	0.417	0.664	0.671
180	0.830	0.876	0.733	0.959	0.987

gles. At 50 eV, the theoretical curve is inside the experimental error for angles $30° \leq \theta \leq 100°$, while at 100 eV, the theoretical curve has a structure in the large angular region not observed in the experiments. For this energy, nevertheless, the cross sections were measured only up to 80°. At the lower energies, effects we have not considered, such as the polarization of the target, could make considerable differences in the cross sections. The outgoing electron, in these cases, is slow enough to feel the long-range polarization potential of the atom. This explains why the results are better for Ne,[20] with polarizability 2.66,[32] than for Ar and Kr with polarizabilities 11.1 and 16.7,[32] respectively.

The FOMBT cross-section curves for the excitation of the states $5s'[\frac{1}{2}]_0^0$ and $5s[\frac{3}{2}]_2^0$ have, in general, the correct order of magnitude and confirm the trend observed in the Ne (Ref. 20) and Ar (Ref. 22) calculations. The reason that the spin-forbidden excitation is not very well described by a first-order theory was first pointed out by Seaton.[33] For optically allowed transitions, a large number of partial waves are required in order to converge the cross section. In this case the low partial waves, which may require a more rigorous treatment that includes coupling and correlation effects, do not significantly contribute to the final results. The differences for allowed transitions between Ne (Ref. 20) on the one hand and Ar (Ref. 22) and Kr on the other arise from the fact that target polarization effects can also influence intermediate partial waves. On the other hand, the spin-forbidden transitions are dominated by low partial waves and therefore are sensitive to the method of calculation employed. In this case polarization is not expected to be the most important effect.

We can also understand this trend from the point of view of the many-body theory. The optically allowed transitions are closer to the single-particle scattering in the sense that the direct process dominates. The spin-

TABLE II. Parameter $\bar{\chi}$ for excitation of $5s'[\frac{1}{2}]_1^0$ of krypton.

Angle (deg)	Incident energy 20 eV	30 eV	50 eV	60 eV	100 eV
10	0.040	0.101	0.155	0.170	0.186
20	0.013	0.147	0.321	0.376	0.416
30	6.180	0.109	0.345	0.405	3.570
40	5.770	5.890	3.810	3.750	3.360
50	4.800	4.350	3.770	3.810	1.310
60	4.130	4.020	3.670	1.660	1.780
70	3.830	3.790	1.540	1.510	1.880
80	3.750	2.970	1.730	1.650	1.790
90	4.430	2.810	2.000	1.760	1.440
100	4.850	3.170	2.210	2.000	0.304
110	4.550	3.530	2.400	2.530	0.433
120	4.180	3.720	2.690	4.200	0.656
130	3.930	3.710	4.720	5.710	0.836
140	3.770	3.580	5.340	6.250	1.360
150	3.680	3.390	5.580	0.346	1.990
160	3.630	3.240	5.830	0.574	1.970
170	3.600	3.150	6.050	0.687	1.810

TABLE III. Parameter Δ for excitation of $5s'[\frac{1}{2}]_1^0$ of krypton.

Angle (deg)	Incident energy 20 eV	30 eV	50 eV	60 eV	100 eV
0	1.570	1.570	1.570	1.570	1.570
10	0.242	0.071	0.030	0.028	0.030
20	0.245	0.117	0.091	0.092	0.129
30	0.400	0.268	0.373	0.663	0.211
40	0.721	0.736	0.534	0.394	0.422
50	0.919	0.753	0.395	0.468	0.388
60	0.805	0.538	0.684	0.923	0.045
70	0.737	0.531	0.398	0.136	0.098
80	0.779	0.509	0.113	0.092	0.165
90	0.834	0.339	0.171	0.178	0.258
100	0.500	0.348	0.242	0.301	0.309
110	0.582	0.373	0.314	0.532	0.169
120	0.638	0.398	0.496	0.945	0.085
130	0.603	0.433	0.725	0.462	0.067
140	0.524	0.445	0.383	0.272	0.099
150	0.431	0.400	0.358	0.200	0.103
160	0.393	0.321	0.396	0.206	0.106
170	0.636	0.420	0.563	0.321	0.149
180	1.570	1.570	1.570	1.570	1.570

forbidden transitions are three-body processes. In a related endeavor, Macek and Alston[34] have demonstrated that the strong second-order Born contribution is important in charge transfer scattering. Their conclusions imply that the inclusion of coupling between channels, which is neglected in the FOMBT, plays a very important role in

TABLE IV. Parameter ϵ for excitation of $5s'[\frac{1}{2}]_1^0$ of krypton.

Angle (deg)	Incident energy 20 eV	30 eV	50 eV	60 eV	100 eV
0	1.570	1.570	1.570	1.570	1.570
10	0.395	0.125	0.049	0.041	0.030
20	0.466	0.231	0.162	0.159	0.228
30	0.789	0.531	0.738	1.290	0.298
40	1.410	1.400	0.924	0.632	0.276
50	1.740	1.330	0.545	0.470	0.265
60	1.460	0.878	0.444	0.342	0.087
70	1.300	0.704	0.305	0.171	0.095
80	1.350	0.605	0.170	0.123	0.171
90	1.400	0.522	0.214	0.249	0.354
100	0.778	0.470	0.332	0.510	0.326
110	0.597	0.450	0.499	1.040	0.129
120	0.574	0.441	0.948	1.780	0.090
130	0.581	0.437	1.320	0.638	0.104
140	0.602	0.441	0.509	0.296	0.190
150	0.645	0.460	0.395	0.231	0.204
160	0.745	0.517	0.446	0.261	0.195
170	1.030	0.732	0.722	0.435	0.252
180	1.570	1.570	1.570	1.570	1.570

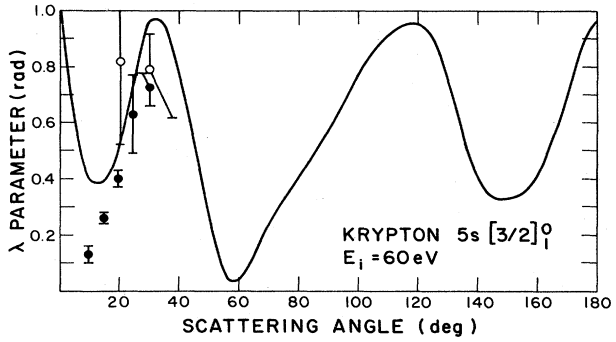

FIG. 12. λ parameter for the $5s[\frac{3}{2}]_1^0$ state of krypton. The experimental data are from McGregor *et al.* (Ref. 10) (○) and from Nishimura *et al.* (Ref. 11) (●).

the pure exchange scattering. Indeed, in recent results for the $2\,^3S$ transition of He,[35] the inclusion of some second-order effects[36,37] in the T matrix caused a dramatic improvement in the DCS.

In Figs. 8 and 9 we compare theoretical curves of the integral cross section with the experimental results of Trajmar *et al.*[5] Although the FOMBT reproduces well the shapes of the curves, our results are too high by factors varying from $\frac{3}{2}$ to 6. This is not unexpected since each experimental ICS was obtained by integration of an extrapolated DCS and considerable error could be introduced in the process. Figures 10 and 11 contain a comparison of the theoretical inelastic momentum-transfer cross sections to the measurements.[5]

The recoupling procedure used in Eqs. (3) and (4) allows us to establish some relation between DCS's of states with $J=2$ and 0. In the previous application[22] the excitation energy for both states was supposed equal. This implied that $\sigma(J=2)/\sigma(J=0)=5$ [see Eqs. (34c) and (34d) in Ref. 22]. Here this assumption is not made but still our results follow the relation in an approximate way. A larger discrepancy from experiments will require different $5s$ functions for each state. For states with $J=1$ there is not such a simple relationship but if we neglect exchange and level splitting, the relation of the DCS is equal to b^2/a^2 [see Eqs. (34a) and (34b) in Ref. 32]. The exchange

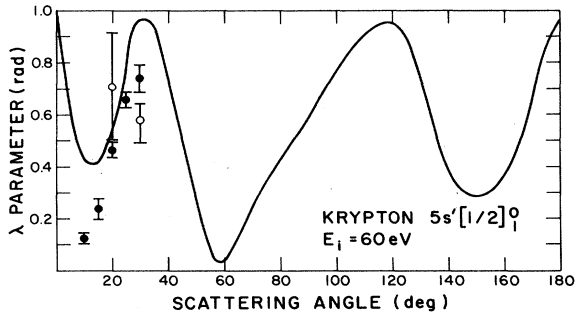

FIG. 13. As Fig. 12, for the $5s'[\frac{1}{2}]_1^0$ state.

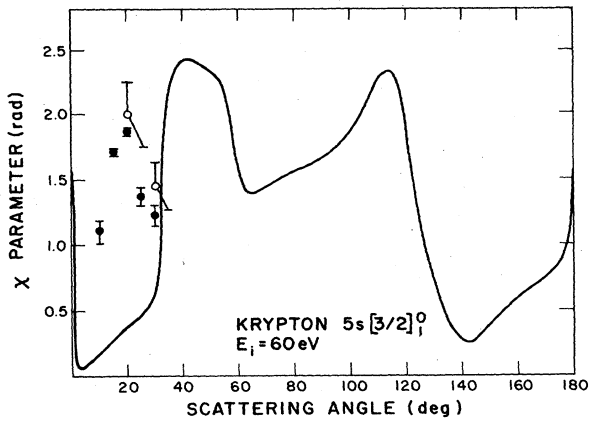

FIG. 14. χ parameter for the $5s[\frac{3}{2}]^0_1$ state of krypton. The experimental data are from McGregor *et al.* (Ref. 10) (○) and from Nishimura *et al.* (Ref. 11) (●).

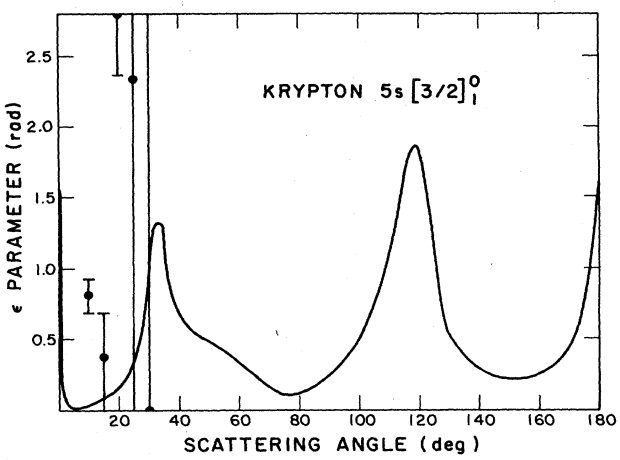

FIG. 16. ϵ parameter for the $5s[\frac{3}{2}]^0_1$ state of krypton. The experimental data are from Ref. 11.

loses its importance as we go to higher energies or small angles.

B. The electron-photon coincidence parameters

Tables I–IV show the results for λ, $\bar{\chi}$, Δ, and ϵ for the states $5s'[\frac{1}{2}]^0_1$ of krypton at the incident energies of 20, 30, 50, 60, and 100 eV. (Tabled results can be obtained from the authors.) We compare our results to the available experimental data[10–12] in Figs. 12–17. The behavior of electron-photon coincidence parameters for Kr is similar to previous results for Ar (Ref. 23) and to a lesser extent to those for Ne.[21] In particular, this atom has a spin-orbit interaction much smaller than Ar or Kr. Δ and ϵ behave at 0° and 180° as dictated by the selection rule[9] and they show some structure due to minima in the magnetic sublevel cross section.[23] For example, the maximum for ϵ corresponds to the minimum for σ_1. $\bar{\chi}$ is now present instead of $|\bar{\chi}|$ as in previous results for Ne and Ar. The reflection symmetry of the scattering plane implies that the angular momentum transferred in the collision lies perpendicular to the scattering plane, and its direction is given by $\sin\bar{\chi}$. Due to our choice of phase convention $0 \leq \bar{\chi} \leq 2\pi$, the jumps in the values of $\bar{\chi}$ correspond to the change of direction of the angular momentum transferred. The figures show that the measurements are in disagreement with each other and with the theoretical results. Nevertheless, the experiments confirm the strong and abrupt structure for the coincidence parameters in the angular region of the measurements, as predicted by the theory. In this case we can expect that a small misalignment in angle could change the experimental data drastically. This could explain the disagreement among the measurements. To better evaluate the quality of our results, it would be necessary to compare with complete experimental curves in a larger angular region.

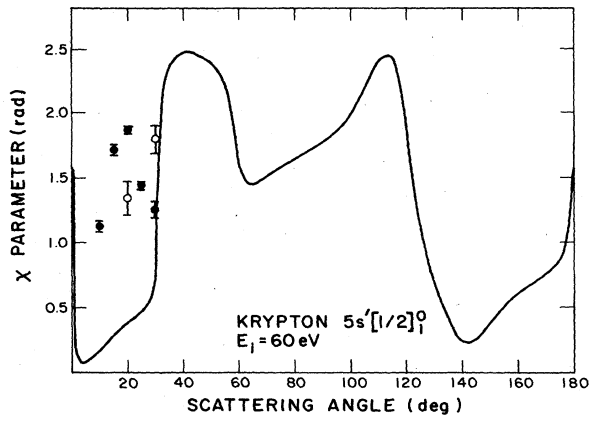

FIG. 15. As Fig. 14, for the $5s'[\frac{1}{2}]^0_1$ state.

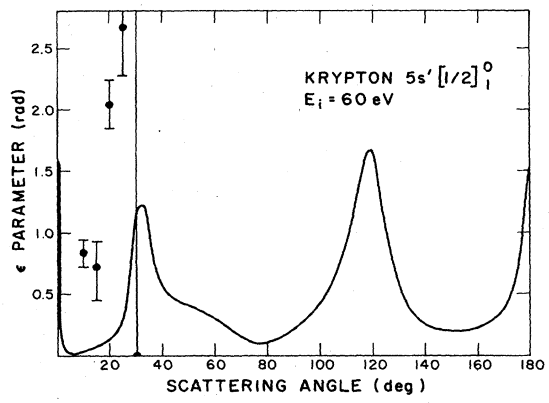

FIG. 17. As Fig. 16, for the $5s'[\frac{1}{2}]^0_1$ state.

Note added in proof. After the completion of this paper, we received revised experimental data from Professor H. Nishimura. Although some of his individual numbers have changed, the general trend continues the same as displayed in the figures, and our analysis remains unchanged.

ACKNOWLEDGMENTS

The authors gratefully acknowledge the joint support of the United States—Latin American Cooperative Science Program, National Science Foundation, and Conselho Nacional de Desenvolvimento Científico e Tecnólogico (CNPq) (Brazil), which made this research possible. One of us (F.J.P.) wants to acknowledge the CNPq (Brazil) for support. Work at Joint Institute for Laboratory Astrophysics (JILA) was supported in part by National Science Foundation Grant No. PHY-82-00805. We thank Gy. Csanak, D. C. Cartwright, L. A. Collins, and D. W. Norcross for valuable discussions and Professor H. Nishimura for permission to quote his results in advance of publication. We also wish to thank L. A. Collins and B. I. Schneider for the use of their linear-algebraic program.

---

*Permanent address: Instituto de Fisica "Gleb Wataghin," Universidade Estadual de Campinas, 13100 Campinas, São Paulo, Brazil.

[1]C. Ramsauer, Ann. Phys. (Leipzig) **72**, 345 (1923).

[2]C. Ramsauer and R. Kollath, Ann. Phys. (Leipzig) **3**, 536 (1929).

[3]B. R. Lewis, E. Weigold, and P. J. O. Teubner, J. Phys. B **8**, 212 (1975).

[4]A. Delage and J. D. Carrete, Can. J. Phys. **53**, 2079 (1975).

[5]S. Trajmar, S. K. Srivastava, H. Tanaka, H. Nishimura, and D. C. Cartwright, Phys. Rev. A **23**, 2167 (1981).

[6]P. S. Ganas and A. E. S. Green, Phys. Rev. A **4**, 182 (1971).

[7]See reviews by K. Blum and H. Kleinpoppen, Phys. Rep. **52**, 203 (1979).

[8]M. Eminyan, K. B. MacAdam, J. Slevin, and H. Kleinpoppen, Phys. Rev. Lett. **31**, 576 (1973).

[9]F. J. da Paixão, N. T. Padial, Gy. Csanak, and K. Blum, Phys. Rev. Lett. **45**, 1164 (1980).

[10]I. McGregor, D. Hils, R. Hippler, N. A. Malik, J. F. Williams, A. A. Zaidi, and H. Kleinpoppen, J. Phys. B **15**, 1411 (1982).

[11]H. Nishimura, A. Danjo, T. Koike, K. Kani, H. Sugahara, and A. Takahashi, in *Electron-Molecule Collisions and Photoionization Processes,* proceedings of the First United States—Japan Seminar, edited by V. McKoy, H. Suzuki, K. Takayanagi, and S. Trajmar (Chemie, Dearfield Beach, Florida, 1982), and private communication.

[12]A. J. Crowe, S. J. King, and P. A. Neill, in Abstracts of the International Symposium on Polarization and Correlation in Electron-Atom Collisions, Münster, West Germany, 1983 (unpublished).

[13]Gy. Csanak, H. S. Taylor, and R. Yaris, Adv. At. Mol. Phys. **7**, 287 (1971); Phys. Rev. A **3**, 1322 (1971).

[14]See P. G. Burke and W. Eissner, in *Atoms in Astrophysics,* edited by P. G. Burke, W. B. Eissner, D. G. Hummer, and I. C. Percival (Plenum, New York, 1983), p. 1.

[15]N. S. Scott, P. G. Burke, and K. Bartschat, in *Abstracts of Papers, Thirteenth International Conference on the Physics of Electronic and Atomic Collisions, Berlin, 1983,* edited by J. Eichler *et al.* (North-Holland, Amsterdam, 1983), p. 103.

[16]L. D. Thomas, Gy. Csanak, H. S. Taylor, and B. S. Yarlagadda, J. Phys. B **7**, 1719 (1974).

[17]A. Chutjian and L. D. Thomas, Phys. Rev. A **11**, 1583 (1975).

[18]H. S. Taylor, A. Chutjian, and L. D. Thomas, in *Electron and Photon Interaction with Atoms,* edited by H. Kleinpoppen and M. R. C. McDowell (Plenum, New York, 1975), pp. 435—444.

[19]G. D. Meneses, N. T. Padial, and Gy. Csanak, J. Phys. B **11**, L237 (1978).

[20]L. E. Machado, E. P. Leal, and Gy. Csanak, Phys. Rev. A **29**, 1811 (1984).

[21]L. E. Machado, E. P. Leal, and Gy. Csanak, J. Phys. B **15**, 1773 (1983).

[22]N. T. Padial, G. D. Meneses, F. J. da Paixão, Gy. Csanak, and D. C. Cartwright, Phys. Rev. A **23**, 2194 (1981).

[23]F. J. da Paixão, N. T. Padial, and Gy. Csanak, Phys. Rev. A **30**, 1697 (1984).

[24]K. Schackert, Z. Phys. **213**, 316 (1968).

[25]R. D. Cowan and K. L. Andrew, J. Opt. Soc. Am. **55**, 502 (1965).

[26]J. C. McConnell and B. L. Moiseiwitsch, J. Phys. B **1**, 406 (1968).

[27]C. Froese-Fischer, Comput. Phys. Commun. **14**, 145 (1978).

[28]J. P. de Jongh and J. van Eck, Physica (Utrecht) **51**, 104 (1971).

[29]G. N. Bates, Comput. Phys. Commun. **8**, 220 (1974).

[30]L. A. Collins and B. I. Schneider, Phys. Rev. A **24**, 2387 (1981).

[31]E. Clementi and C. Roetti, At. Data Nucl. Data Tables **14**, 177 (1974).

[32]H. Margenau and N. R. Kestner, *Theory of Intermolecular Forces,* 2nd ed. (Pergamon, New York, 1971), p. 38.

[33]M. J. Seaton, Proc. Phys. Soc. London **77**, 174 (1961).

[34]J. Macek and S. Alston, Phys. Rev. A **26**, 250 (1982).

[35]F. J. da Paixão and G. D. Meneses (unpublished).

[36]F. J. da Paixão, Ph.D. thesis, Universidade Estadual de Campinas, 1980.

[37]Gy. Csanak, H. S. Taylor, and D. N. Tripathy, J. Phys. B **6**, 2040 (1973).